Available online at www.sciencedirect.com
ScienceDirect
Journal of Photochemistry and Photobiology A: Chemistry 190 (2007) 301–309
Journal of Photochemistry and Photobiology A:Chemistry
www.elsevier.com/locate/jphotochem

The role of Ag(I) ions in the electronic spectroscopy of adenine–cytosine mispairs A MS-CASPT2 theoretical study

Marko Schreiber, Leticia González *

Freie Universität Berlin, Institut für Chemie und Biochemie, Takustraβe 3, 14195 Berlin, Germany

Received 14 November 2006; received in revised form 19 January 2007; accepted 31 January 2007
Available online 6 February 2007

Abstract

Adenine–cytosine (AC) mispairs have been theoretically studied with MS-CASPT2//CASSCF methods in the presence and absence of Ag ions. The electronically excited states of the most stable AC mispair in the reverse-Wobble (RW) conformation have been compared with those of different Ag(I)–AC complexes, including (i) metalated RW conformations, and (ii) the most stable structures in gas phase which contain the Ag ion bridging A and C. The spectra of these complexes are characterized by charge-transfer (CT) and strong locally excited (LE) states. The metal-to-metal, metal-to-ligand, and Rydberg transitions are very weak in comparison to the nucleobase transitions. Attending to the LE and CT states, and except for the shifts induced by the presence of the Ag, the electronic spectrum of metalated AC mispairs resembles the one of the RW, showing two intense LE bands around 4.5 and 5.5 eV, corresponding to transitions within the adenine and cytosine π-system, respectively. Additionally TD-DFT results obtained with the B3LYP functional are compared with MS-CASPT2//CASSCF calculations. The results clearly evidence the weakness of TD-DFT to describe long range exchange interactions leading to strongly underestimated CT states.

Keywords: DNA; Adenine; Cytosine; Silver; Excited states; CASPT2; TD-DFT

1. Introduction

Since many years, quantum chemical methods have spurred the study of the electronic structure of nucleic acids and related model compounds [1–3]. With the advent of femtosecond time-resolved experiments, a rich amount of photochemical and photophysical information about DNA constituents accumulates, stimulating the calculation of electronic excited states [4]. Nowadays, the interpretation of electronic spectra is supported by reliable excitation energies and oscillator strengths of nucleic bases [5–9], which help understanding the ultrafast excited state dynamics and relaxation mechanisms of DNA [10–14]. The spectra of the nucleic acids consist of rather broad bands that strongly overlap. The excitation energies of the strong absorption lines are well known experimentally [4]. Recent calculations of excited state properties of the nucleobases and base pairs provided plenty of information concerning weak transitions and spectral changes due to possible structural isomers or tautomers. The importance of tautomers different from the canonical ones (those involved in the Watson–Crick pairing [15]) has been recognized early [16]. It is therefore very important to determine which tautomers are responsible for a particular experiment.

The occurrence of mispairs- or base pair mismatches-reduces the accuracy of DNA replication. The mispairing of adenine (A) and cytosine (C) may break Chargaff's rule that the amount of adenine or guanine (G) is approximately equal to thymine (T) or cytosine (C), respectively [17]. Just a few studies are reported for adenine–cytosine (AC) mispairs [17,18]. NMR experiments propose two possible structural models of the duplex [19]: one involving two hydrogen bonds, and another with a single hydrogen bond [17]. With two hydrogen bonds, there are two energetically favorable pairing models for AC base pairs: the reverse Wobble (RW) and the reverse Hoogsteen, the former predicted to be a bit more stable than the later [1,20,21]. The stability of the hydrogen bonds in the charged reverse Wobble and reverse Hoogsteen AC mispairs have been

* Corresponding author. Tel.: +49 30 838 52097.
E-mail address: leti@chemie.fu-berlin.de (L. González).

1010-6030/$ – see front matter © 2007 Elsevier B.V. All rights reserved.
doi:10.1016/j.jphotochem.2007.01.035

studied with density functional theory (DFT) by Tian [21]. Our research interest is focused on the appearance of mispairs in DNA and the question whether their occurrence is supported by metal cations. Metal ions are known to have mutagenic effects. They can stabilize rare nucleobase tautomers, which are then no longer compatible with the formation of Watson–Crick base pairs [22]. Heavy metal ions, such as Ag(I), are strong nucleic acid binders and form ternary complexes with nucleobases, nucleosides, nucleotides, and other ligands [23]. Interestingly, some of the Ag(I)–containing DNA complexes exhibit antibacterial activity [24], but details of the binding mode of Ag(I) in the Ag-polynucleotides are unclear [25]. Nevertheless, it is well accepted [26] that Ag(I) has a distinct preference for binding to endo-cyclic ring nitrogen atoms of the heterocyclic bases of DNA, in contrast to most divalent cations (such as Mg(II), Mn(II), and Co(II)), which interact preferably with the backbone phosphates or the sugar moieties [27].

Binding of Ag(I) is necessarily accompanied by UV absorption changes. Therefore, the analysis of electronic transition energy shifts in nucleobases compared to experimental values can provide valuable information about the probabilities of metal ion binding to different reaction centers. Ag(I) chelates of adenine, for instance, are predicted as the most stable conformations in gas phase [28,29]. On the contrary, the interpretation of the solution UV-absorption spectrum of Ag complexes in comparison to that of isolated adenine [19], points to the existence of monodentated adenine complexes [30]. The inclusion of metals in DNA mispairs can also influence the photophysical and photochemical properties of DNA and reveal novel relaxation pathways.

In this paper, we study the effect of Ag(I) on AC mispairing. We have determined the low-lying excited states and corresponding oscillator strengths of silver-metalated AC mispairs and compared the UV-absorption features to those of the AC mispair itself, as well as to those of the isolated nucleobase tautomers which build the corresponding mispair. The rest of the paper is organized as follows. The details of the calculations can be found in Section 2. Section 3 describes the different type of base pair structures for which the electronic excitations are calculated and discussed; first those without metal ions, followed by the metalated ones. A summary is given in Section 4.

2. Computational details

For the presented calculations four types of compounds (see Fig. 1) have been considered: (i) the reverse Wobble AC mispair (**1**), (ii) Ag(I)–AC mispairs in four conformations (**2**–**5**), (iii) complexes of the N9H tautomer of adenine with Ag(I) in three possible binding positions at Nl, N3 and N7 (**6**–**8**), and (iv) a chelate Ag(I)–cytosine complex (**9**). All the structures have been optimized using the MP2 approximation. The MWB relativistic core potential for the silver [31] and the cc-pVTZ basis set for the other atoms have been employed for all structures, except for the Ag(I) mispairs (**2**–**5**), where the cc-pVTZ scheme was replaced with cc-pVDZ.

To describe the electronic spectra of the above systems, the state averaged complete active space SCF (SA-CASSCF) method [32,33] was used and supplemented with multi-state second order perturbation theory (MS-CASPT2), which includes dynamic σ–π polarization effects [34–36]. To avoid intruder states in the CASPT2 calculations a level shift of 0.3 a.u. was used [37,38]. The CAS state interaction method, CASSI, was used to compute transition moments [39,40]. To calculate oscillator strengths, the transition dipole moments obtained with perturbatively modified CASSCF wave functions were combined with MS-CASPT2 excitation energies.

For the calculation of the excited states the full electron basis sets of atomic natural orbital (ANO-RCC) type are used [41]. The basis set includes correlation of the semi-core orbitals, effectively mixing the core correlating, polarization and valence correlating functions among the ANO's. For silver the basis set is contracted to 6s5p3d1f. For other heavy atoms and hydrogen the double-ζ contraction has been applied (3s2p1d/2s1p). Scalar relativistic effects have been included using a Douglas–Kroll Hamiltonian [42,43].

In the CASSCF calculations, the set-up of the active space is always a non-trivial issue. To ensure comparability, the active space needs to guarantee consistent wavefunctions for all model systems. In the case of metalated base pairs, at least the strong covalent binding Ag-ligand valence orbitals, containing a significant metal d contribution, should be set active [44]. This implies that, in principle, the active space should include all π- and n-type orbitals of the nucleobases, plus the 4d- and Rydberg 5s orbitals of the silver atom. This leads to an active space of more than 30 orbitals and electrons, respectively, impracticable from the computational point of view. To select the most important orbitals, exploratory time-dependent TD-DFT [45–47] calculations, using the B3LYP functional [48–50] and the D95* basis set [51] with the MWB core potential, were performed. Independent of the validity of the method (see Section 3 for further discussion) the following singlet excitations have been found: local and charge transfer $\pi \rightarrow \pi^*$ transitions (LE($\pi_a\pi_a^*$), LE($\pi_c\pi_c^*$) and CT($\pi_a\pi_c^*$), for local excited states within either monomer, and charge transfer states between the bases), $n \rightarrow \pi^*$, $\pi \rightarrow 5s$ and $4d_{z^2} \rightarrow 5s$ transitions. It is obvious that, to describe these excitations with a CASSCF wavefunction, the active space should contain the orbitals involved in such transitions. To reduce the size of the active space, we performed several tests which indicated that, (i) the $n \rightarrow \pi^*$ states are higher in energy than LE and CT excited states; therefore, n-type orbitals have been excluded from the active space, and (ii) the lowest energy π-orbitals can be kept inactive. Thus, the active space has been restricted to the two highest occupied and two lowest unoccupied π-orbitals located at the respective nucleobase, i.e. four π- and π*-orbitals located on adenine and four π- and π*-orbitals located on cytosine. Including the $4d_{z^2}$-type and 5s orbitals of the Ag, where $4d_{z^2}$ describes a covalent bonding orbital between silver and the respective nitrogen/oxygen atom at the nucleobase, an active space of 10 orbitals with 10 active electrons has been used. With this, a reasonable compromise between computation time and reproducible set-ups of the active space for the different molecules has been found. The excitation energies for **1** have been computed using state-averaged (SA)-CASSCF(8,8) over six roots with equal weights (denoted as SA(6)-CASSCF(8,8)),

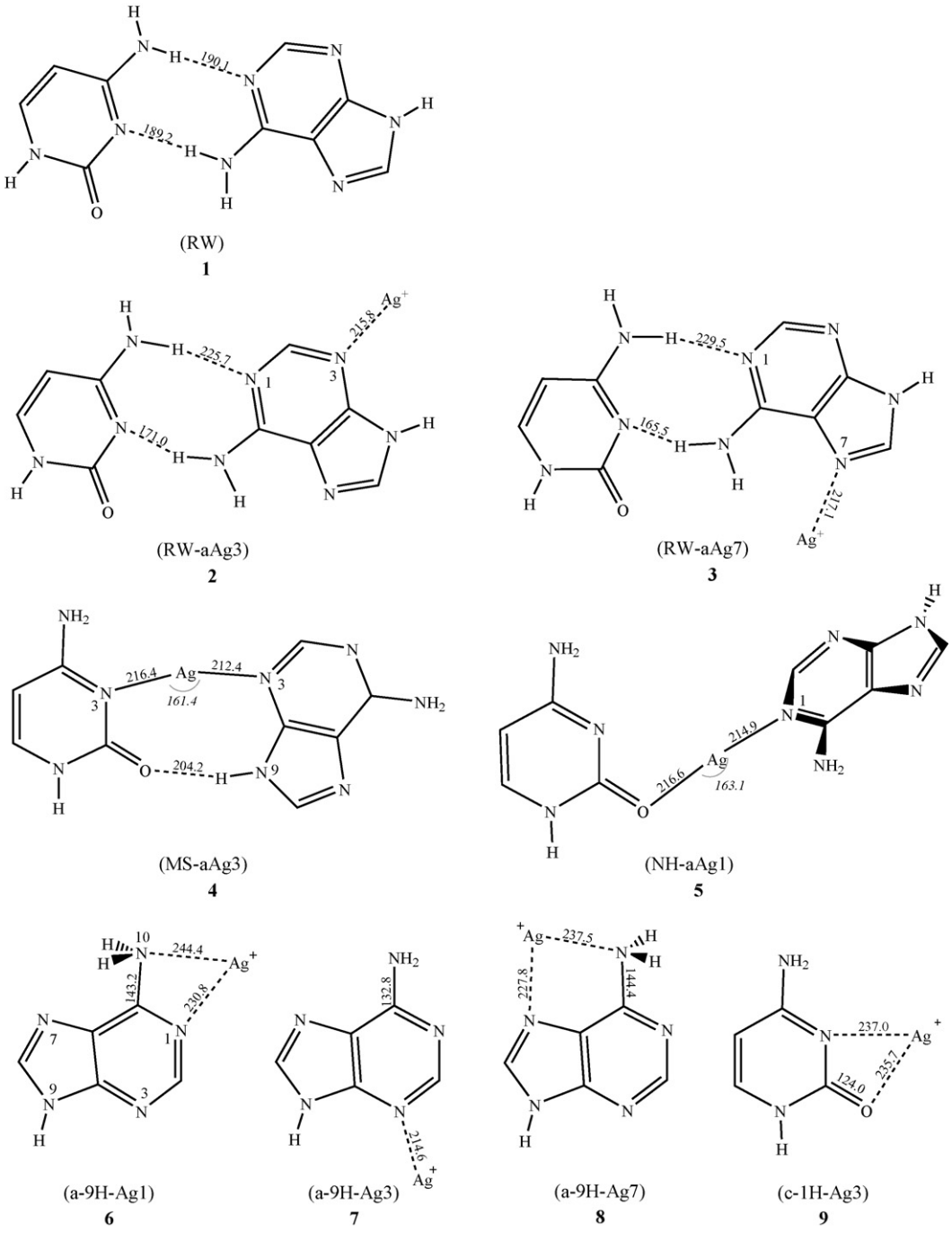

Fig. 1. Ground state equilibrium structures of the reverse Wobble AC mispair (**1**), Ag(I)–AC mispairs in four conformations (**2–5**), complexes of the N9H tautomer of adenine with Ag(I) in three possible binding positions at Nl, N3 and N7 (**6–8**), and the Ag(I)–cytosine complex (**9**). The optimizations have been performed at the MP2/cc-pVTZ (**1**, **6–9**) and the MP2/cc-pVDZ (**2–5**) level of theory. Bond lengths are given in (pm), angles in (°).

whereas for the complexes **2–5** 10 averaged roots are computed, SA(10)-CASSCF(10,10). For the monomer complexes the active space and the number of calculated singlet states has been adjusted accordingly, i.e. SA(6)-CASSCF(6,6).

To the best of our knowledge, no excited states calculation on silver complexes using multiconfigurational methods have been reported. The CASSCF, MS-CASPT2, and CASSI calculations were performed with the MOLCAS-6 software [52]. The MP2 geometry optimizations and TD-DFT excited states calculations were performed with the GAUSSIAN03 program [53]. Unless otherwise indicated, the discussed energies and energy differences are MS-CASPT2.

3. Results and discussion

3.1. Ground state geometries

All the geometries for which the electronic excited states are calculated and discussed below are collected in Fig. 1. Structure **1** is the reverse Wobble (RW) AC mispair, which consists of the

canonical adenine and cytosine tautomers joined by two hydrogen bonds of about 190 pm. In agreement with previous findings [1,21], a planar structure has been found.

Structures **2**–**5** are different models for Ag-metalated mispairs. The complexes **2** and **3** are based on the reverse Wobble AC base pair, with a silver ion attached to the free binding positions on adenine, N3 in **2** and N7 in **3**. Even if the arrangements **2** and **3** could appear as the most probable metalated structures (since they are based on the RW mispair), they are energetically unfavourable. A thorough investigation of Ag(I) AC mispairs [29] revealed that in gas phase these complexes are much higher in energy (ca. 40 kcal/mol) than the most stable (MS) Ag(I)–AC mispair **4**. In **4** the silver ion is located in a bridging position between the two nucleobases. Note that this complex is set-up from the respective canonical adenine and cytosine tautomers. The hydrogen at N9 of adenine exhibits a hydrogen bond with the O7 of cytosine. Since this hydrogen substitutes for a possible glycosidic bond in biological systems this model is of rather theoretical nature, only valid for isolated systems in the gas phase. This is different from the metalated mispair **5**, which exhibits no hydrogen bond (NH) between the adenine and cytosine nucleobases. Here the silver bridges between adenine and cytosine by binding to Nl of adenine and O7 of cytosine. Due to the absence of hydrogen bonds, this type of structures are very flexible and not planar. Close in energy to the minimum structure (3.9 kcal/mol) [29], with the endocyclic nitrogen positions in adenine and cytosine free for possible glycosidic bonds, arrangement **5** may also occur in biological systems.

In order to understand the shifts induced when going from free bases to the base pairs, the tautomers of adenine and cytosine nucleobases with Ag(I) in the same position as in the mispair have been also considered. The structures **6**–**9** are limited to the canonical tautomers of A and C since only those appear in the studied AC mispairs, allowing for a direct comparison. The Ag(I)–adenine complexes **6** and **8** are chelate where the silver binds to the N10 of the amino group and to Nl or N7, respectively. As a part of an AC mispair, however, the silver either forms a single bond with A (like in **3**) or bridges between A and C (like in **5**). In the cytosine complex **9** the silver chelates between the endocylic Nitrogen and the carbonyl Oxygen. Again, in the dimers **4** and **5**, the Ag chelate to C is replaced for the benefit of a bridging between both nucleobases. Monomer **7**, on the other hand, has Ag in a monodentated fashion at position N3, as found also in the mispairs **2** and **4**. A complete survey of Ag(I)–adenine and Ag(I)–cytosine complexes, including the canonical, but also rare tautomers which can be stabilized by the presence of a metal ion, can be found in Ref. [30].

3.2. Vertical excitation energies of the AC reverse Wobble mispair

The vertical excitation energies of the complex RW **1** have been determined using a planar ground state geometry in C_1 symmetry. The calculated vertical excitation energies of the six low-lying $^1A_1$ states, with their corresponding dipole moments, oscillator strengths and dominating configuration are given in Table 1. All calculated states correspond to $\pi \rightarrow \pi^*$ transitions, which can be classified as local excitations (LE) within a particular monomer or as charge-transfer (CT) excitations between the bases. In parenthesis the excitation energies, dipole moments and oscillator strengths for the respective monomers calculated with CASSCF(6,6) are given. The obtained results for the adenine monomer are in qualitative agreement with those obtained by Fülscher and coworkers [5,6], regarding the relative order of the states. Energetically, the energy gap between the local states of adenine is about 0.4 eV, while in Refs. [5,6], as well as in others, see e.g. [54,55], this gap lies between 0.1 and 0.2 eV. The size of the active space as well as the basis set are responsible for this difference, as clearly illustrated in Ref. [30].

Table 1
MS-CASPT2//SA(6)-CASSCF(8,8) vertical excitation energies ΔE (eV), dipole moments μ (D) and oscillator strengths f of the lowest singlet states of the reverse Wobble base pair (RW, **1**), obtained at the ground state MP2/cc-pVTZ geometry

State	ΔE	μ	f
S_0	–[a]	6.31	–
$1^1LE(\pi_a\pi_a^*)$	4.72 (5.05)	3.50 (2.78)	0.35 (0.01)
$2^1LE(\pi_c\pi_c^*)$	4.92 (4.57)	4.46 (4.82)	0.25 (0.16)
$3^1LE(\pi_a\pi_a^*)$	5.34 (5.49)	4.18 (3.28)	0.09 (0.16)
$4^1LE(\pi_c\pi_c^*)$	5.73 (6.16)	3.76 (3.72)	0.13 (0.02)
$1^1CT(\pi_a\pi_c^*)$	6.42	24.67	0.01

The numbers in parenthesis denote the values for the respective monomers.
[a] The ground state energy is −860.57142792 a.u.

The lowest singlet state of the AC base pair has LE character (1^1LE) and involves π-electronic excitation within the adenine chromophore. This is followed by a LE-state involving π-electronic excitation within the cytosine, and another two LE states localized within adenine and cytosine, respectively. In view of the oscillator strengths, the 1^1LE and 2^1LE are the most important absorbing states, calculated at 4.72 and 4.92 eV, respectively. The excitation energies of these states can be compared with the excitation energies of the lowest $\pi \rightarrow \pi^*$ singlet states of the monomers calculated at the same level of theory (see Table 1). Even if energetically, our values have an error bar of a couple of tenths of electron volt, this error should be similar in adenine and AC mispairs, so that the following analysis is helpful. In adenine, mispairing with cytosine stabilizes the lowest $\pi_a \rightarrow \pi_a^*$ singlet state by about 0.33 eV, while the dipole moment increases noticeably. The lowest LE ($\pi_c \rightarrow \pi_c^*$) state of cytosine ($2^1$LE), on the other hand, is blue shifted by 0.35 eV due to mispairing, whereas the dipole moment decreases slightly. The next LE states, originating in the adenine and cytosine π-system (3^1LE and 4^1LE) are red-shifted by 0.15 and 0.43 eV, with respect to the adenine and cytosine monomers, respectively.

The shifts found for the lowest LE transition are similar to those found by Sobolewski and Domcke [10] or Wesolowski [56] in the complexation of guanine with cytosine in the GC Watson–Crick base pair: the lowest LE state of cytosine is destabilized by 0.4 eV [10] or 0.3 eV [56] upon dimerization with guanine. The $n \rightarrow \pi^*$ state (not reported here) of cytosine is destabilized by twice as much [56]. Surprisingly, the excited states of adenine and thymine are much less affected when paired

in the WC AT base pair. Wesolowski [56], as well as Perun and coworkers [13] have observed a red-shift of the LE($\pi_a\pi_a^*$) transition in adenine due to the complexation with thymine amounting to about 0.1 eV [13]. In the present AC mispair, this transition is also red-shifted, but to a larger extent (0.33 eV).

The fifth singlet excited state of AC is identified as a CT state at 6.42 eV. This state reflects a π-electron transfer from adenine to cytosine, where the respective π and π* orbitals are completely localized on either base. The charge separation is reflected by the very high dipole moment (24.13 D) of this transition and a very small oscillator strength. This state appears at a similar energy in the AT base pair (6.26 eV) [13], but lower in energy in the GC base pair, which has been calculated below 5 eV [10].

3.3. Vertical excitation energies of the metalated AC base pairs

Taking the electronic spectrum of **1** as a reference, we shall compare here the differences in the excited states induced by the presence of the silver cation. As mentioned above, we have done TD-DFT (B3LYP) calculations in order to assess the applicability of the TD-DFT method compared to CASSCF/MS-CASPT2 calculations, and classify the character of the states that can occur in the four model systems **2**–**5**. Exemplarily, the results obtained for the MS complex **4** are shown in Fig. 2.

Twelve electronically excited states have been calculated with TD-DFT, color-coded depending on the nature of the transition: CT (red), LE within the adenine or the cytosine chromophore (black), $\pi_a \rightarrow 5s$ (green), metal-to-ligand $4d_{z^2} \rightarrow \pi^*_{a/c}$ (cyan), metal-to-metal $d_{z^2} \rightarrow 5s$ (blue) and $n \rightarrow \pi^*_{a/c}$ (orange). Based on these states, the active space for the CASSCF calculations has been set-up to include 10 electrons in 10 orbitals, describing the lowest energy transitions. Of course, since the application of different methods can induce a reordering of the states, different trials have been carried out to guarantee that no low-lying state is missing at the MS-CASPT2 level of theory.

As seen in Fig. 2, TD-DFT predicts the CT state as the lowest in energy at 3.4 eV, followed by a Rydberg $\pi_a \rightarrow 5s$ transition at 4.12 eV, a $4d_{z^2} \rightarrow \pi^*_{a/c}$ transition at 4.43 eV, and an additional CT state at 4.67 eV. The LE states are calculated higher in energy at about 4.8 eV. It is well-known that standard TD-DFT can yield substantial errors for CT and Rydberg excited states due to the lack of long range exchange interactions [57,58]. Encouraging steps to remedy these problems can be found in Refs. [59,60]. A quick glance to the reordering of the states obtained with CASSCF and MS-CASPT2 theories indicates that in these type of systems, TD-DFT drastically underestimates the CT and Rydberg states. Even if the energies at CASSCF level of theory are much too high, the CT state is clearly pushed above the LE and the Rydberg states. Also noticeable is that the $4d_{z^2} \rightarrow \pi^*_{a/c}$ and $n \rightarrow \pi^*_{a/c}$ states do not appear under the 10 lowest CASSCF/CASPT2 states. As expected, the inclusion of dynamical correlation with MS-CASPT2 shifts all states to the red with respect to the CASSCF energies. Nevertheless, except for the Rydberg $\pi_a \rightarrow 5s$ states, the states keep the CASSCF energy ordering. That is, the first singlet excited state possesses

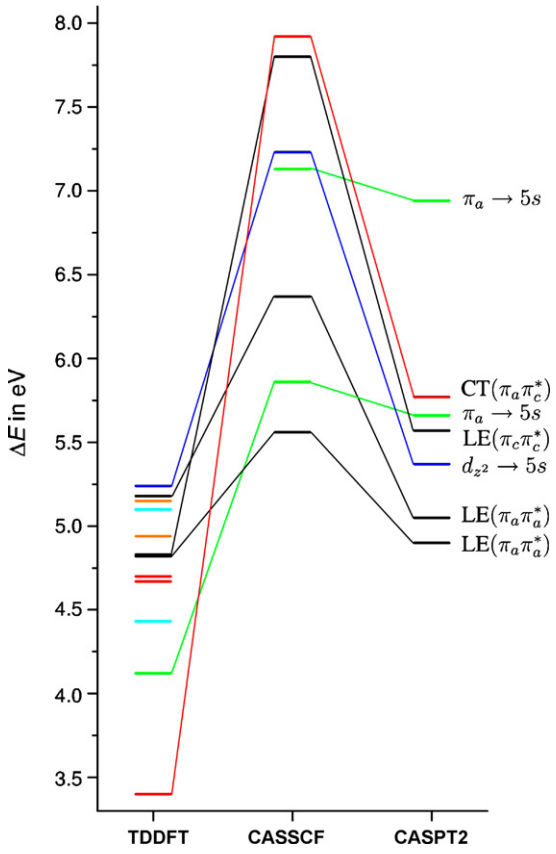

Fig. 2. Comparison of the electronic excited states of **4** calculated at different levels of theory. The states are color-coded depending on the nature of the transition: CT (red), LE within the adenine or the cytosine chromophore (black), $\pi_a \rightarrow 5s$ (green), metal-to-ligand $4d_{z^2} \rightarrow \pi^*_{a/c}$ (cyan), metal-to-metal $d_{z^2} \rightarrow 5s$ (blue) and $n \rightarrow \pi^*_{a/c}$ (orange).

LE character while the CT state is much higher in energy. The comparison of these results with the TD-DFT values leads to the conclusion that the application of TD-DFT (B3LYP) for metalated DNA mispairs is not adequate. Henceforth we shall focus on MS-CASPT2 results.

The vertical excitation energies and oscillator strengths for the complexes **2**–**5** are collected in Table 2. The states are arranged according to the nature of the transitions: Rydberg $\pi_a \rightarrow 5s$, metal-to-metal $4d_{z^2} \rightarrow 5s$, LE and CT states. To resolve the origin of the observed absorptions, the excited states of the underlying building blocks, i.e. of the corresponding monomer-silver complexes of the N9H tautomer of adenine and N1H tautomer of cytosine, are presented in Table 3. For the sake of clarity, the most important states of all Ag(I)-monomers and mispairs **1**–**9** have been graphically correlated in Fig. 3.

From Tables 2 and 3 one can see that the Rydberg and metal-to-metal states have zero or negligible oscillator strengths. Thus, the LE states are the dominating absorption bands of the metalated compounds. Despite their small transition probability, πσ* states of Rydberg character have been postulated to be of great importance for explaining the photostability mechanism of bare nucleobases [11]. In order to infer the role of the $4d_{z^2} \rightarrow 5s$ Rydberg states in the metalated AC mispairs we have focused on the MS-aAg3 structure, which shows a considerable $4d_{z^2} \rightarrow 5s$

Table 2
MS-CASPT2//SA(10)-CASSCF(10,10) vertical excitation energies ΔE (eV) and oscillator strengths f of the lowest singlet states of the metalated AC base pairs **2**–**5**, obtained at the ground state MP2/cc-pVDZ geometries

State	RW-aAg3 (**2**)		RW-aAg7 (**3**)		MS-aAg3 (**4**)		NH-aAgI (**5**)	
	ΔE	f	ΔE	f	ΔE	f	ΔE	f
S_0	–[a]	–	–[b]	–	–[c]	–	–[d]	–
$\pi \rightarrow$ 5s transitions								
$\pi_a \rightarrow$ 5s	2.95	0.00	2.89	0.00	5.66	0.00	6.23	0.00
$\pi_c \rightarrow$ 5s	4.56	0.00	4.50	0.00	–	–	–	–
$\pi_a \rightarrow$ 5s	4.65	0.00	4.65	0.00	6.94	0.00	7.67	0.00
$d_{z^2} \rightarrow$ 5stransitions								
$d_{z^2} \rightarrow$ 5s	3.97	0.07	4.24	0.03	5.37	0.09	6.26	0.17
$\pi \rightarrow \pi^*$ transitions								
1^1LE($\pi_a\pi_a^*$)	4.39	0.30	4.49	0.38	4.90	0.25	5.00	0.01
2^1LE($\pi_a\pi_a^*$)	5.62	0.02	5.47	0.01	5.05	0.02	5.23	0.24
3^1LE($\pi_c\pi_c^*$)	5.70	0.44	5.75	0.43	5.57	0.44	5.29	0.62
1^1CT($\pi_a\pi_c^*$)	–	–	–	–	5.77	0.02	7.29	0.00

[a] The ground state energy is −6172.69751738 a.u.
[b] The ground state energy is −6172.69807112 a.u.
[c] The ground state energy is −6172.76791016 a.u.
[d] The ground state energy is −6172.76724275 a.u.

Table 3
MS-CASPT2//SA(6)-CASSCF(6,6) vertical excitation energies ΔE (eV) and oscillator strengths f of the lowest singlet states of the adenine/cytosine-monomer silver-complexes **6**–**9**

State	a-9H-AgI (**6**)		a-9H-Ag3 (**7**)		a-9H-Ag7 (**8**)		c-1H-Ag3 (**9**)	
	ΔE	f	ΔE	f	ΔE	f	ΔE	f
S_0	–[a]	–	–[b]	–	–[c]	–	–[d]	–
$d_{z^2} \rightarrow$ 5s	4.18	0.01	4.26	0.01	4.24	0.01	4.25	0.00
1^1LE($\pi\pi^*$)	4.75	0.29	4.60	0.40	4.86	0.30	5.12	0.31
$\pi \rightarrow$ 5s	5.01	0.00	3.50	0.00	5.16	0.00	4.94	0.00
2^1LE($\pi\pi^*$)	6.00	0.24	5.64	0.04	6.37	0.21	5.75	0.15
$\pi \rightarrow$ 5s	6.36	0.00	4.96	0.00	6.44	0.00	5.26	0.00

[a] The ground state energy is −5778.50344919 a.u.
[b] The ground state energy is −5778.50331906 a.u.
[c] The ground state energy is −5778.50897075 a.u.
[d] The ground state energy is −5706.31297910 a.u.

transition, see Table 2. The $4d_{z^2}$ and 5s orbitals build the bonding between the Ag and the corresponding ligands, therefore, state correlation diagrams along both dissociation ligand paths have been constructed using the vertical excitation energies

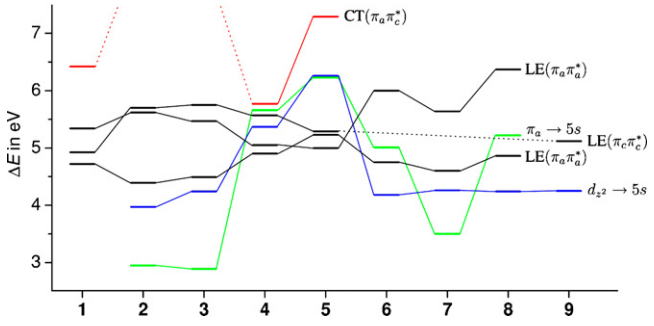

Fig. 3. Correlation of the most important electronic excited states of the model systems **1**–**9**. The states are color-coded depending on the nature of the transition: CT (red), LE within the adenine or the cytosine chromophore (black), $\pi_a \rightarrow$ 5s (green) and metal-to-metal $d_{z^2} \rightarrow$ 5s (blue).

of **4** at the equilibrium and at the asymptotic A − Ag + C and A + AgC channels. From Fig. 4 can be seen that different crossings between the Rydberg and LE states occur before dissociation can take place. In contrast to what it is observed in the bare nucleobases [10,13], no crossing with the electronic ground state is observed along these particular coordinates.

The presence of the metal induces energetic shifts in the LE (blue) and CT (red) states, as it can be seen in Fig. 3. Note that, the overall energetic splitting in the LE states is systematic within a particular type of metalated mispair, but different if one refers to the RW-based (structures **2** and **3**) or the MS **4** and NH **5** type of structures. Moreover, the states involving transitions to the metal appear below the LE states in the case of **2** and **3** but above them in the case of **4** and **5**.

Recall that in the non-metalated RW structure **1** the absorbing states are the two lowest LE($\pi \rightarrow \pi^*$) states-one localized in A, the other in C-whereas higher LE states have weaker oscillator strengths (cf. Table 1). This trend can also be observed in the mispairs **2**–**5**: the absorbing states are the lowest LE($\pi \rightarrow \pi^*$)

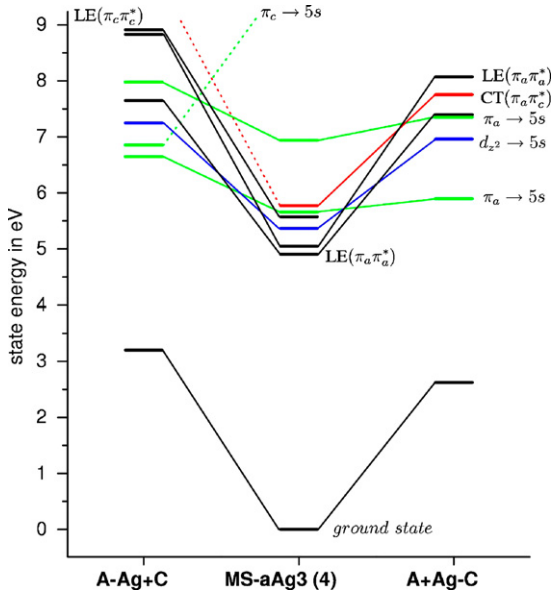

Fig. 4. State correlation diagrams of **4** along the ligand dissociation A-Ag + C and A + Ag-C channels. For dissociation, the fragments are considered at a distance of 500 pm, keeping the rest of the molecule frozen. The states are color-coded depending on the nature of dominating configurations: CT (red), LE within the adenine or the cytosine chromophore (black), $\pi_a \rightarrow 5s$ or $\pi_c \rightarrow 5s$ (green) and metal-to-metal $d_{z^2} \rightarrow 5s$ (blue).

states localized in either monomer (see Table 2). The strong LE states of the RW mispair **1** are predicted at 4.72 eV (localized in adenine) and 4.92 eV (localized in cytosine). In the metalated RW base pairs **2**–**3** the lowest $\pi_a \rightarrow \pi_a^*$ state (1^1LE) is red-shifted to 4.39 eV (**2**) and 4.49 eV (**3**), while the lowest $\pi_c \rightarrow \pi_c^*$ (3^1LE) is strongly blue-shifted to 5.70 eV (**2**) and 5.75 eV (**3**). If we compare these excitations with those of the corresponding monomers, we can see that the 1^1LE($\pi_a \rightarrow \pi_a^*$) states are red-shifted by 0.2–0.3 eV with respect to the Ag-adenine complexes **7** and **8**, while the 3^1LE($\pi_c \rightarrow \pi_c^*$) states are red-shifted by more than 1 eV with respect to the cytosine monomer. In the MS and NH silver complexes the energy shifts with respect to the non-metalated RW structure are different: the band corresponding to the $\pi_a \rightarrow \pi_a^*$ transition is blue-shifted to 4.90 eV (**4**) and to 5.23 eV (**5**), while the band assigned as $\pi_c \rightarrow \pi_c^*$ is also blue-shifted to 5.57 eV (**4**) and 5.29 eV (**5**). Systematically, these energies are also red-shifted with respect to the monomers by about 0.2–0.5 eV (see Tables 2 and 3). The 3^1LE($\pi_c \rightarrow \pi_c^*$) state in **5** is close to that of the metalated monomer **9** (5.12 eV), indicated by a dotted line in Fig. 3.

Note that while the 3^1LE($\pi_c \rightarrow \pi_c^*$) state is the same in all complexes **1**–**5**, the lowest LE($\pi_a \rightarrow \pi_a^*$) state is not. This can be easily spotted by inspecting the oscillator strengths. In the adenine-containing complexes **1**–**4** and **6**–**8** the lowest energy LE($\pi_a \rightarrow \pi_a^*$) state shows a strong absorption, indicated by oscillator strengths of about 0.3–0.4. However, the respective oscillator strength of **5** is close to zero. The second state with LE($\pi_a \rightarrow \pi_a^*$) character in **5**, on the other hand, has an oscillator strength of 0.24, while these are close to zero for this state in the other mispairs. This indicates that at the employed level of theory there is a state switch, which is supported by the analysis of the involved orbitals: in **4** the 1^1LE($\pi_a \rightarrow \pi_a^*$) state is dominated by a single configuration describing an excitation from the HOMO to the LUMO orbital, $\pi_H \rightarrow \pi_L$ (60%), while the second 2^1LE($\pi_a \rightarrow \pi_a^*$) state consists of two configurations ($\pi_{H-1} \rightarrow \pi_L$, 27%, and $\pi_H \rightarrow \pi_{L+1}$, 38%). In **5** it is the other way round (1^1LE($\pi_a \rightarrow \pi_a^*$): $\pi_{H-1} \rightarrow \pi_L$, 24%, and $\pi_H \rightarrow \pi_{L+1}$, 51%; 2^1LE($\pi_a \rightarrow \pi_a^*$): $\pi_H \rightarrow \pi_L$, 76%).[1] This state switch can be neither directly related to the binding position of the silver (Nl of adenine in this case), since the a-9H-Agl (**6**) complex shows the same ordering of the LE($\pi_a \rightarrow \pi_a^*$) states as all other metalated monomers and base pairs, nor to the hydrogen bonding (see Table 3). Noticeable is that the gap between the 1^1LE and 2^1LE states in the MS and NH structures is ca. 0.2 eV, as in adenine itself [5], whereas in the RW structures goes beyond 1 eV. Similar large gaps are also found in the metalated free adenine bases **6**–**8**.

Like in the WC base pairs, the LE states within the cytosine chromophore are in general more affected by the base pairing than those of adenine. While for RW the lowest LE($\pi_c \rightarrow \pi_c^*$) is, compared to the c-lH monomer, already shifted to the blue, this state is further destabilized due to the metalation. The addition of silver shifts this band into the region above 5 eV, with differences of 0.2–0.5 eV with respect to **9**, depending on the mispair.

The CT state (red) in **4** and **5** mispairs is, like the CT state in the RW base pair **1**, dominated by a $\pi_a \rightarrow \pi_c^*$ transition (with contributions of 71% and 87% in **4** and **5**, respectively). In **4** it is predicted at 5.77 eV, stabilized by about 0.7 eV with respect to the CT state in the RW base pair, and not very different from the position of the CT state in the AT base pair (6.26 eV) [13]. In the GC base pair, however, the CT($\pi_g \rightarrow \pi_c^*$) state appears much lower in energy, at 4.75 eV [10]. In the linear non-hydrogen bonded complex **5** the CT state is blue-shifted to 7.29 eV. Note that in the metalated RW base pairs **2** and **3** the CT state does not appear within the 10 calculated roots.

Even if the transitions in which the 5s orbital of the metal are involved are not very intense, they are clearly influenced by the binding position of the silver (cf. Fig. 3). In some cases they can be related to experimental spectral data: when the silver coordinates to one of the free binding sites of adenine or cytosine (**2**, **3** and **6**–**9**), the $d_{z^2} \rightarrow 5s$ (blue) transition appears around 4 eV. Despite its weak oscillator strength, this transition has been assigned [30] to the long tail of the experimental spectrum of Ag-adenine observed between 3.5 and 4.3 eV [19]. In all the calculated Ag–adenine complexes this state is calculated between 4.0 and 4.3 eV, in agreement with the experimental band. In the mispairs, this transition is heavily affected when the ion bridges between the nucleobases, that is, in complexes **3** and **4**, where the band is strongly blue-shifted (to 5.37 eV in **3** and to 6.26 eV in **4**). This shift is inherent to the Ag-bridging mispairs, since in the monomers and in the RW base pairs this state is not affected, regardless of whether the ion is bound in a mono- or bi-dentated fashion (compare, e.g. **6** with **8**). The $\pi_a \rightarrow 5s$ (green) transitions also strongly depend on the Ag binding condition. On the

[1] The fact that the $\pi_H \rightarrow \pi_L$ transition is higher in energy is also known for the adenine monomer itself [11,30].

one hand, a bidentated binding of the silver allows for a back-donation to the adenine π-system, causing a stabilization of the ground state. This, on the other hand, goes at the expense of the $\pi_a \rightarrow 5s$ state, which is heavily influenced by a destabilized 5s orbital. Thus for monodentated Ag-complexes (**2**, **3**, and **7**) this state appears below 4 eV, strongly red-shifted with respect to the chelate structures.

4. Summary

Multiconfigurational MS-CASPT2//CASSCF calculations have been used to explore the UV absorption spectra of adenine–cytosine (AC) mispairs in the gas phase. From the different conformations in which AC mispairs are known to exist, the reverse-Wobble (RW) is the most stable one in gas phase. In the presence of Ag, different structures can be obtained, RW ones in which Ag is attached to the free binding sites in adenine, but also others where Ag can bridge the two nucleobases [29]. Four species including the most stable conformers in each family have been selected to analyze the electronic excited states. The resulting vertical electronic excitations, corresponding dipole moments and oscillator strengths of the mispairs are compared with the monomers that assemble the mispair.

The absorption spectrum of the RW AC mispair is characterized by a series of locally excited (LE) $\pi \rightarrow \pi^*$ states centered at the A or C calculated between 4.7 and 4.9 eV, as well as a charge transfer (CT) state predicted at 6.4 eV. The most intense transitions are the two lowest LE states, taking place within the adenine or cytosine π-system, respectively. These states are shifted with respect to the corresponding band in adenine and cytosine monomers, where the shift for the cytosine LE state appears to be more pronounced.

The inclusion of Ag in the AC mispairs enriches the UV spectra with weak metal-to-metal, metal-to-ligand and Rydberg excitations besides the stronger LE and weak CT states. In general, for all the metalated complexes investigated herein, the position of the LE states is similar to that found in the RW AC mispair. Analogously to the RW mispair, amongst the low-lying LE states, two of them are very intense. One is localized in the adenine π-system and is predicted between 4.4 and 5.2 eV, depending on the metalated complex. The other is localized in cytosine and can be found around 5.2–5.7 eV. Compared to the monomers, the shifts are larger for LE($\pi_c \rightarrow \pi_c^*$) excitations. In all complexes the CT state appears above the LE states. Unlike the LE and CT states, the transitions involving the metal ion are significantly affected by the binding position of the Ag.

In conclusion, the photochemistry and photophysics of the metalated mispairs appears to be dominated by the locally excited states at the nucleobases and the charge transfer state between them. Similar results could be expected in other metalated DNA complexes with filled d shell metals.

The electronic excitations have also been computed with TD-DFT (B3LYP) in order to assess its performance in this type of complexes. As it has been found in other systems [57,58], TD-DFT dramatically underestimates the energy of the long-range CT states. The LE states, however, differ by only about 0.2 eV.

Acknowledgements

This research is financed by the SFB 450 "Analysis and Control of Ultrafast Photoinduced Reactions". The European COST Action P9 "Radiation Damage in Biomolecular Systems" is also acknowledged. L.G. thanks the "Berliner Programm zur Förderung der Chancengleichheit für Frauen in Forschung und Lehre".

References

[1] P. Hobza, J. Šponer, Chem. Rev. 99 (1999) 3247.
[2] J. Šponer, P. Hobza, Collect. Czech. Chem. Commun. 68 (2003) 2231.
[3] P. Jurečka, J. Šponer, J. Černý, P. Hobza, Phys. Chem. Chem. Phys. 8 (2006) 1985.
[4] C. Crespo-Hernández, B. Cohen, P. Hare, B. Kohler, Chem. Rev. 104 (2004) 1977.
[5] M.P. Fülscher, B.O. Roos, J. Am. Chem. Soc. 117 (1995) 2089.
[6] M.P. Fülscher, L. Serrano-Andrés, B.O. Roos, J. Am. Chem. Soc. 119 (1997) 6168.
[7] M. Shukla, J. Leszczynski, J. Phys. Chem. A 106 (2002) 4709.
[8] M. Shukla, J. Leszczynski, J. Comput. Chem. 25 (2002) 768.
[9] C. Marian, D. Nolting, R. Weinkauf, Phys. Chem. Chem. Phys. 7 (2005) 3306.
[10] A.L. Sobolewski, W. Domcke, Phys. Chem. Chem. Phys. 6 (2004) 2763.
[11] C. Marian, J. Chem. Phys. 122 (2005) 104314.
[12] M. Shukla, J. Leszczynski, J. Phys. Chem. A 109 (2005) 7775.
[13] S. Perun, A. Sobolewski, W. Domcke, J. Phys. Chem. A 110 (2006) 9031.
[14] L. Blancafort, J. Am. Chem. Soc. 128 (2006) 210.
[15] J. Watson, F. Crick, Nature 171 (1953) 737.
[16] R. Wilson, P. Callis, Photochem. Photobiol. 31 (1980) 323.
[17] M.H. Sarma, G. Gupta, R.H. Sarma, R. Bald, U. Engelke, S. Oei, R. Gessner, V. Erdmann, Biochemistry 26 (1987) 7707.
[18] W. Hunter, T. Brown, N. Anand, O. Kennard, Nature 320 (1986) 552.
[19] A.Y. Rubina, Y.V. Rubin, V.A. Sorokin, M.K. Shukla, J. Leszczynski, Polish J. Chem. 79 (2005) 1873.
[20] J. Šponer, P. Jurečka, P. Hobza, J. Am. Chem. Soc. 126 (2004) 10142.
[21] S. Tian, J. Phys. Chem. A 109 (2005) 5153.
[22] J. Müller, R. Sigel, B. Lippert, J. Inorg. Biochem. 79 (2000) 261.
[23] S. Tyagi, S. Gencaslan, U. Singh, J. Chem. Eng. Data 48 (2003) 925.
[24] Z. Guo, P. Sadler, Angew. Chem. Int. Ed. 38 (1999) 1512.
[25] H. Arakawa, J. Neault, H. Tajmir-Riahi, Biophys. J. 81 (2001) 1580.
[26] J. Šponer, M. Sabat, J. Burda, J. Leszczynski, P. Hobza, B. Lippert, J. Biol. Inorg. Chem. 4 (1999) 537.
[27] H. Sigel, Chem. Soc. Rev. (1993) 255.
[28] A.K. Vrkic, T. Taverner, P.F. James, R.A.J. O'Hair, Dalton Trans. (2004) 197.
[29] M. Schreiber, L. González, J. Comp. Chem. 2007, in press.
[30] M. Schreiber, L. González, Chem. Phys. Lett. 435 (2007) 136.
[31] D. Andrae, U. Häussermann, M. Dolg, H. Stoll, H. Preuss, Theor. Chim. Acta 77 (1990) 123.
[32] B.O. Roos, P.R. Taylor, P.E.M. Siegbahn, Chem. Phys. 48 (1980) 157.
[33] B.O. Roos, Int. J. Quant. Chem. S14 (1980) 175.
[34] K. Andersson, P.-Å. Malmqvist, B.O. Roos, A.J. Sadlej, K. Wolinski, J. Phys. Chem. 94 (1990) 5483.
[35] K. Andersson, P.-Å. Malmqvist, B.O. Roos, J. Chem. Phys. 96 (1992) 1218.
[36] J. Finley, P.-Å. Malmqvist, B.O. Roos, L. Serrano-Andrés, Chem. Phys. Lett. 288 (1998) 299.
[37] B.O. Roos, K. Andersson, Chem. Phys. Lett. 245 (1995) 215.
[38] B.O. Roos, K. Andersson, M.P. Fülscher, L. Serrano-Andrés, K. Pierloot, M. Merchán, V. Molina, J. Mol. Struct. Theochem. 388 (1996) 257.
[39] P.Å. Malmqvist, B.O. Roos, Chem. Phys. Lett. 155 (1989) 189.
[40] P.-Å. Malmqvist, B.O. Roos, B. Schimmelpfennig, Chem. Phys. Lett. 357 (2002) 230.
[41] B.O. Roos, R. Lindh, P.-Å. Malmqvist, V. Veryazov, P.-O. Widmark, J. Phys. Chem. A 109 (2005) 6575.

[42] M. Douglas, N. Kroll, Ann. Phys. 82 (1974) 89.
[43] B. Hess, Phys. Rev. A 33 (1986) 3742.
[44] K. Pierloot, Mol. Phys. 101 (2003) 2083.
[45] M.E. Casida, C. Jamorski, K.C. Casida, D.R. Salahub, J. Chem. Phys. 108 (1998) 4439.
[46] R. Stratmann, G. Scuseria, M. Frisch, J. Chem. Phys. 109 (1998) 8218.
[47] K. Wiberg, R. Stratmann, M. Frisch, Chem. Phys. Lett. 297 (1998) 60.
[48] A.D. Becke, Phys. Rev. A 38 (1988) 3098.
[49] A.D. Becke, J. Chem. Phys. 98 (1993) 5648.
[50] C. Lee, W. Yang, R.G. Parr, Phys. Rev. B 37 (1988) 785.
[51] T.H. Dunning, P.J. Hay, Modern Theoretical Chemistry, Plenum Press, New York, 1976.
[52] G. Karlström, R. Lindh, P.-Å. Malmqvist, B.O. Roos, U. Ryde, V. Veryazov, P.-O. Widmark, M. Cossi, B. Schimmelpfennig, P. Neogrady, L. Seijo, Comput. Mater. Sci. 28 (2003) 222.
[53] M.J. Frisch, G.W. Trucks, H.B. Schlegel, G.E. Scuseria, M.A. Robb, J.R. Cheeseman, J.A. Montgomery Jr., T. Vreven, K.N. Kudin, J.C. Burant, J.M. Millam, S.S. Iyengar, J. Tomasi, V. Barone, B. Mennucci, M. Cossi, G. Scalmani, N. Rega, G.A. Petersson, H. Nakatsuji, M. Hada, M. Ehara, K. Toyota, R. Fukuda, J. Hasegawa, M. Ishida, T. Nakajima, Y. Honda, O. Kitao, H. Nakai, M. Klene, X. Li, J.E. Knox, H.P. Hratchian, J.B. Cross, V. Bakken, C. Adamo, J. Jaramillo, R. Gomperts, R.E. Stratmann, O. Yazyev, A.J. Austin, R. Cammi, C. Pomelli, J.W. Ochterski, P.Y. Ayala, K. Morokuma, G.A. Voth, P. Salvador, J.J. Dannenberg, V.G. Zakrzewski, S. Dapprich, A.D. Daniels, M.C. Strain, O. Farkas, D.K. Malick, A.D. Rabuck, K. Raghavachari, J.B. Foresman, J.V. Ortiz, Q. Cui, A.G. Baboul, S. Clifford, J. Cioslowski, B.B. Stefanov, G. Liu, A. Liashenko, P. Piskorz, I. Komaromi, R.L. Martin, D.J. Fox, T. Keith, M.A. Al-Laham, C.Y. Peng, A. Nanayakkara, M. Challacombe, P.M.W. Gill, B. Johnson, W. Chen, M.W. Wong, C. Gonzalez, J.A. Pople, Gaussian 03, Revision C.02, Gaussian, Inc., Wallingford, CT, 2004.
[54] S. Perun, A.L. Sobolewski, W. Domcke, J. Am. Chem. Soc. 127 (2005) 6257.
[55] L. Serrano-Andrés, M. Merchán, A.C. Borin, Chem. Eur. J. 12 (2006) 6559.
[56] T.A. Wesolowski, J. Am. Chem. Soc. 126 (2004) 11444.
[57] A. Dreuw, M. Head-Gordon, J. Am. Chem. Soc. 126 (2004) 4007.
[58] A. Dreuw, M. Head-Gordon, Chem. Rev. 105 (2005) 4009.
[59] T. Yanai, D.P. Tew, N.C. Handy, Chem. Phys. Lett. 393 (2004) 51.
[60] O. Gritsenko, E.J. Baerends, J. Chem. Phys. 121 (2004) 655.